Copyright WILEY-VCH Verlag GmbH & Co. KGaA, 69469 Weinheim, Germany, 2016.

ADVANCED FUNCTIONAL MATERIALS

Supporting Information

for *Adv. Funct. Mater.*, DOI: 10.1002/adfm.201602808

Multifunctional Photonics Nanoparticles for Crossing the Blood–Brain Barrier and Effecting Optically Trackable Brain Theranostics

Ajay Singh, Woong Kim, Youngsun Kim, Keunsoo Jeong, Chi Soo Kang, YoungSoo Kim, Joonseok Koh, Supriya D. Mahajan, Paras N. Prasad, and Sehoon Kim**

Copyright WILEY-VCH Verlag GmbH & Co. KGaA, 69469 Weinheim, Germany, 2013.

Supporting Information

Multifunctional Photonics Nanoparticles for Crossing the Blood-Brain Barrier and Effecting Optically Trackable Brain Theranostics

Ajay Singh, Woong Kim, Youngsun Kim, Keunsoo Jeong, Chi Soo Kang, YoungSoo Kim, Joonseok Koh, Supriya D. Mahajan, Paras N. Prasad, and Sehoon Kim**

Dr. A. Singh, Dr. W. Kim, Y. Kim, Dr. K. Jeong, Dr. C. S. Kang, Dr. Y. Kim, Dr. S. Kim
Center for Theragnosis and Center for Neuro-Medicine, Korea Institute of Science and Technology (KIST), Seoul 136-791, Korea
E-mail: sehoonkim@kist.re.kr

Dr. A. Singh, Prof. P. N. Prasad
Institute for Lasers, Photonics and Biophotonics, Department of Chemistry, State University of New York, Buffalo, NY 14260, USA
E-mail: pnprasad@buffalo.edu

Prof. J. Koh
Department of Organic and Nano System Engineering, Konkuk University, Seoul 143-701, Korea

Prof. S. D. Mahajan
Department of Medicine, Division of Allergy, Immunology, and Rheumatology, State University of New York, Clinical Translational Research Center, Buffalo, NY 14203, USA

Supplementary Schemes and Figures

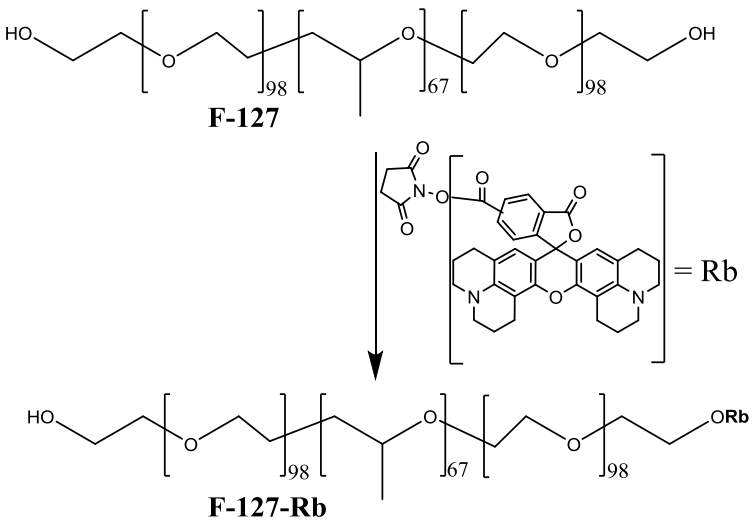

Scheme S1. Chemical structure and synthetic route of F-127-Rh.

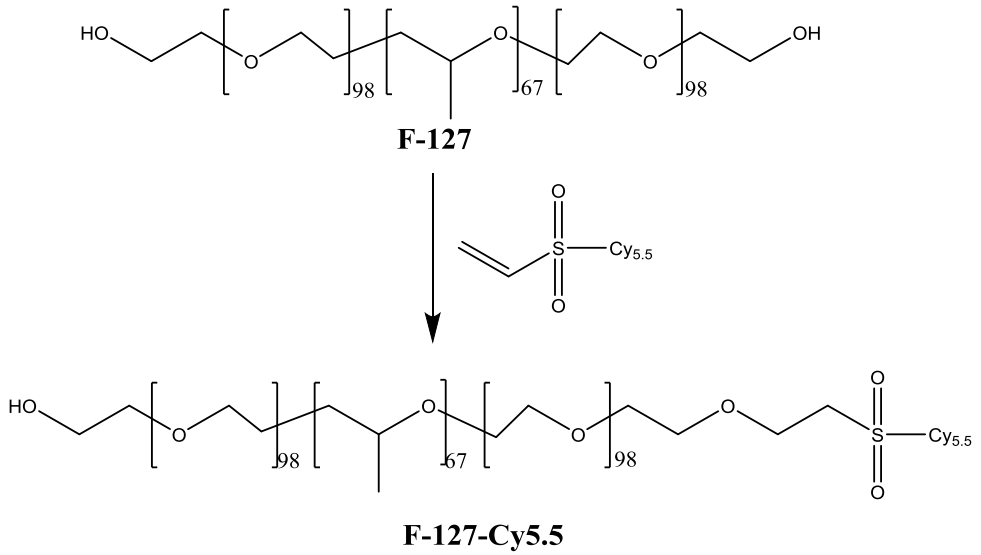

Scheme S2. Chemical structure and synthetic route of F-127-Cy5.5.

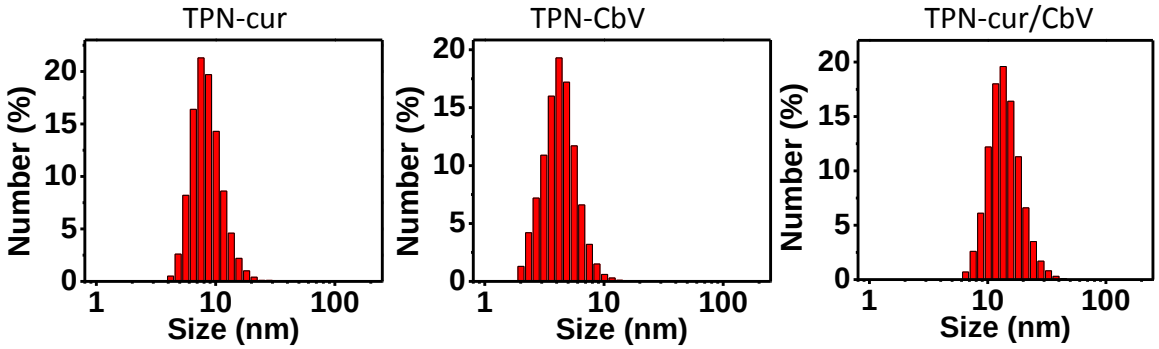

Figure S1. Number-averaged hydrodynamic size distributions of TPNs.

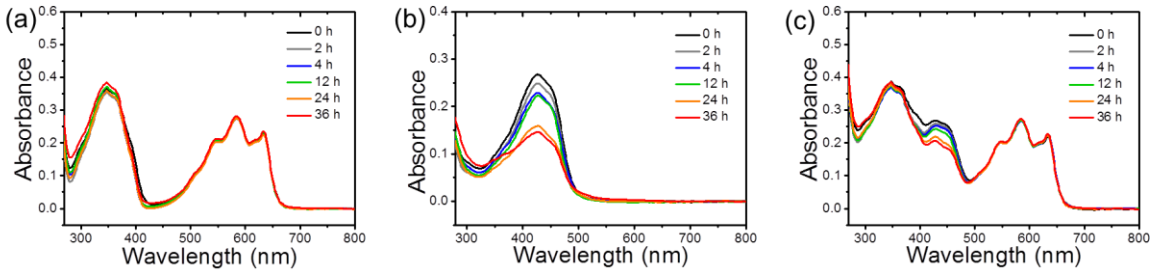

Figure S2. Temporal evolution of absorption spectra: (a) TPN-CbV, (b) TPN-cur, and (c) TPN-CbV/cur. Each TPN was diluted with buffer (PBS, pH 7.4) by ten times and incubated at 37 ^{o}C.

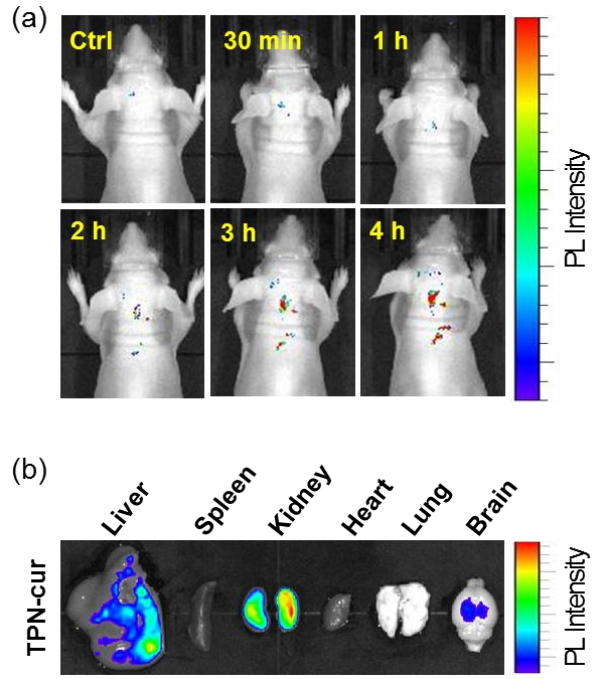

Figure S3. (a) *In vivo* fluorescence imaging of temporal signals from free curcumin (10 μg of curcumin in 20 μL of DMSO) intraperitoneally injected to a normal mouse. (b) *Ex vivo* fluorescence image of major organs resected at 4 h post-injection of free curcumin. A filter set (Excitation: 500 nm, Emission: 570 nm) was used for the fluorescence images.

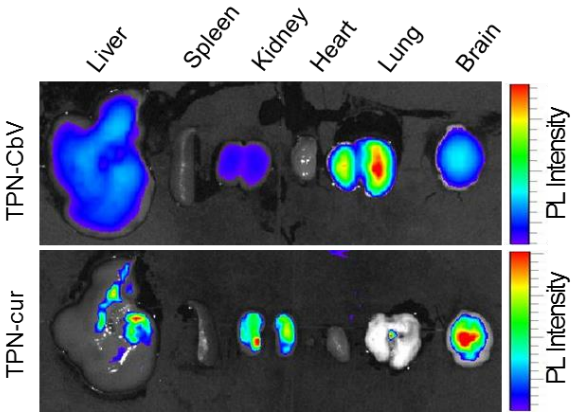

Figure S4. *Ex vivo* fluorescence images of major organs resected at 4 h post-injection of TPN-cur and TPN-CbV (n = 3). Filter sets: TPN-cur (λex = 500 nm, λem = 570 nm), TPN-CbV (λex = 640 nm, λem = 710 nm). In case of TPN-CbV, the most intense signal was found at lung, indicating the lung-favorable accumulation of TPN-CbV.

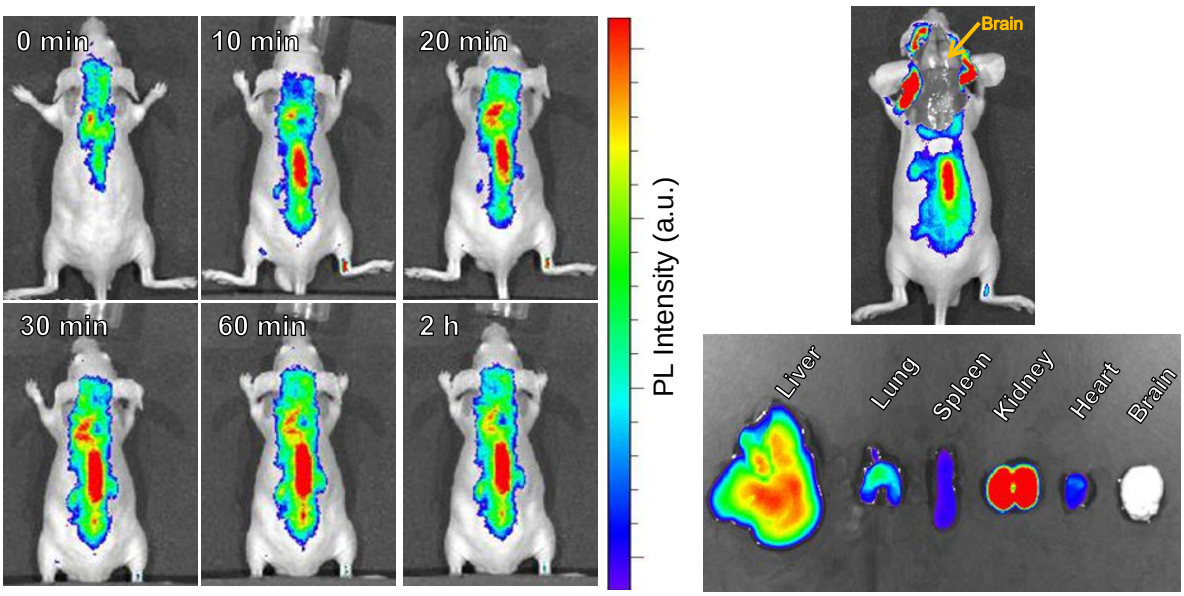

Figure S5. (left) *In vivo* imaging of temporal signals from F-127-Cy5.5 intravenously injected to normal mice, and (right) *ex vivo* images of the sacrificed body and major organs resected at 4 h post-injection. Imaging time points are indicated in the *in vivo* images.

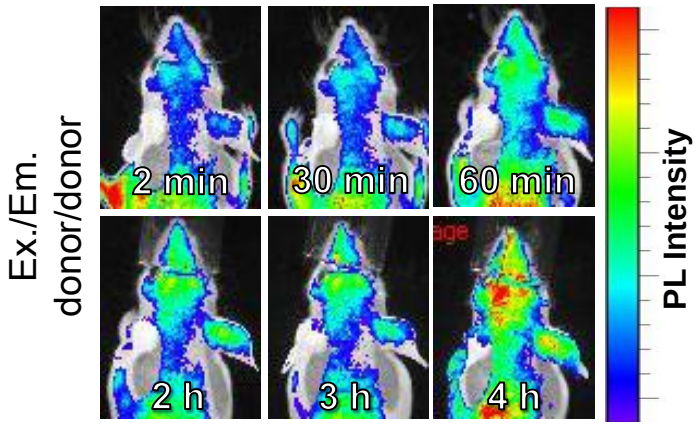

Figure S6. *In vivo* imaging of temporal signals from TPN-cur/CbV intravenously injected to normal mice. Excitation/emission wavelengths are (a) 500 nm/540 nm (directly excited curcumin emission).

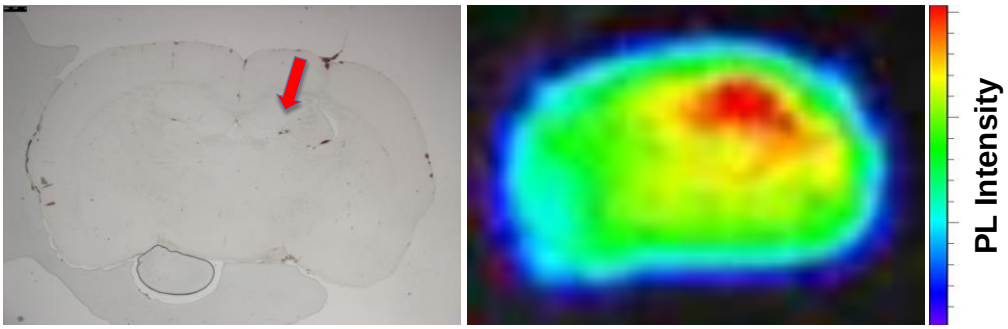

Figure S7. Optical (left) and fluorescence (right) images of brain section. The red arrow indicates the GBM xenograft in the brain. In the right image, the fluorescence signal of TPN-CbV at 700 nm was taken under excitation at 640 nm.

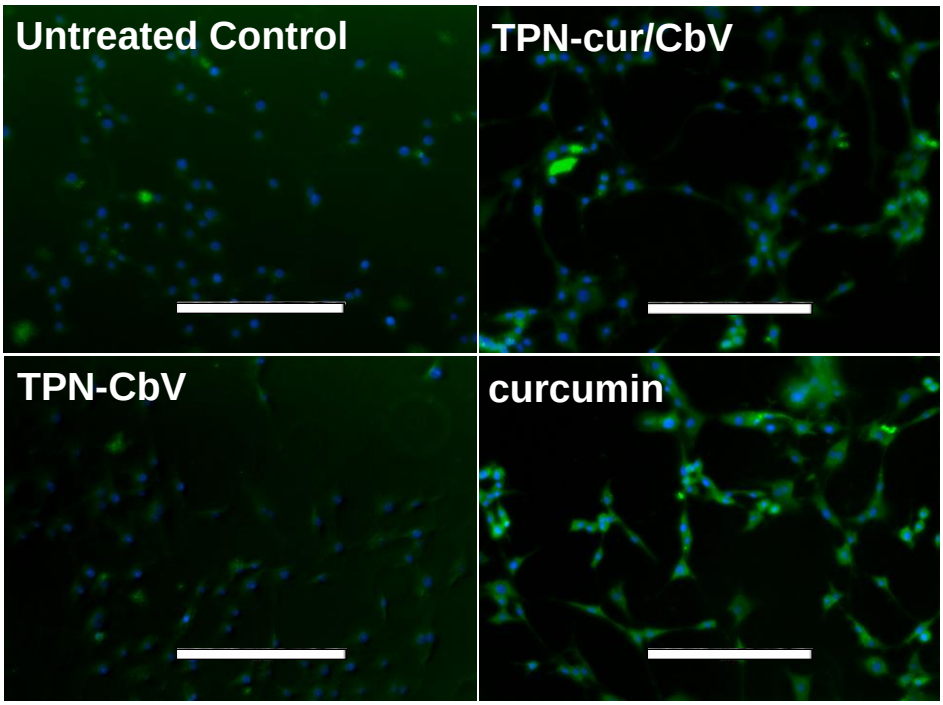

Figure S8. Immunostaining of pro-apoptotic BCL-xS expressed in rat C6 malignant glioma cells treated with TPN-CbV, curcumin, and TPN-cur/CbV. Scale bars: 200 μm.

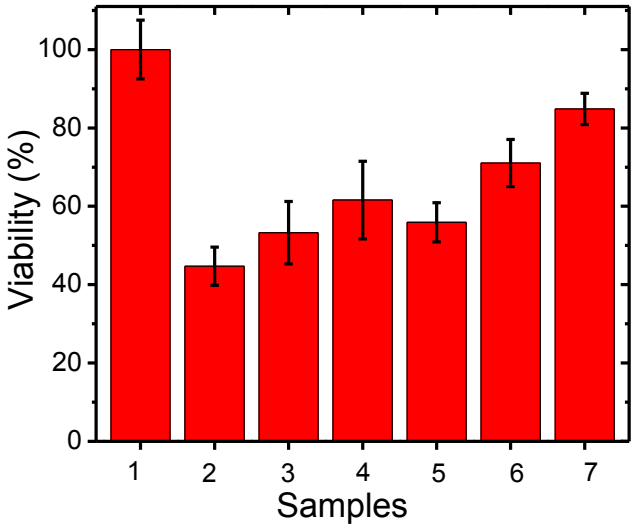

Figure S9. *In vitro* MTT assay showing cytotoxicity of TPN-cur and TPN-cur/CbV at concentrations of 20 mg/mL with varying volumes: (1) control (F-127), (2) TPN-cur (100 µL), (3) TPN-cur (50 µL), (4) TPN-cur (10 µL), (5) TPN-cur/CbV (100 µL), (6) TPN-cur/CbV (50 µL), (7) TPN-cur/CbV (10 µL).